

# Effect of variable permeability on convection in porous media

Fiaz Ur Rehman and Andy Woods \*

**Abstract** In this paper, we study the effect of varying permeability on convection in porous media. The basic mathematical framework for convection in porous media governed by Darcy's Law is outlined. The linear stability analysis is performed to observe convection patterns. The resulting mathematical model is solved by implementing `bvp4c` in Matlab. In the classical case where permeability is constant, we observe symmetric contours of Bénard convection cells and the critical Rayleigh number is  $Ra_c = 4\pi^2$  with wave number  $a = \pi$ . As permeability is varied, the critical Rayleigh number and wave number changed. Also the Bénard convection cells are not symmetric in the non-classical setting. We also plotted contours for temperature  $\theta$  and stream function  $\psi$ .

## 1 Introduction

This paper is focused on convection in porous media, which has many applications in geophysical fluid dynamics. In volcanic systems, geothermal circulation controls the transportation of sediments, minerals, and heat transport through porous rocks [1]. Natural convection is one of the three processes of heat transfer which occurs in both liquids and gases due to the density differences caused by temperature variations. When a layer of viscous fluid is heated from below, the density of the fluid is decreased and it tends to rise due to buoyancy forces. As the hotter fluid

---

Fiaz Ur Rehman  
School of Mathematics, Monash University, Victoria 3800, Australia  
e-mail: fiaz.urrehman@monash.edu

Andy Woods  
Earth Science Department, University of Cambridge, UK  
e-mail: aww1@cam.ac.uk

\* This report presents the results of a project undertaken by the first author at the Matrix Workshop *Instabilities in Porous Media*, April 3-23, 2024, under the supervision of the second author.

rises, it displaces cooler fluid and begins to rise, creating a continuous circulation pattern known as a convection cell. On the other hand, cooler fluid is denser compared to the hotter fluid, so cooler fluid tends to sink, leading to a downward-flowing convection cell. These convection cells are also known as Bénard convection cells. If a saturated porous layer is heated from below, instability occurs which leads to these convection cells [3, 4]. Modelling such phenomena is helpful for understanding geothermal convection.

There has been a lot of work related to convection in porous media [5–10]. In this paper, we are interested in understanding the effect of varying permeability on convection in porous media.

## 2 Mathematical modelling

Consider a saturated layer of porous salt rock as shown in Fig. 1. The layer is confined between  $0 \leq z \leq h$ . Let the layer be heated uniformly from below and its temperature is  $T_0 + \Delta T$  at  $z = 0$ . On the other side of the layer, the boundary is cooler with temperature  $T_0$  at  $z = h$ .

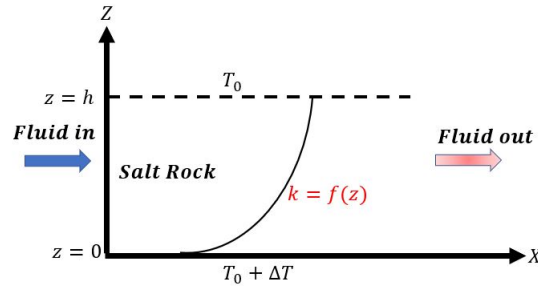


Fig. 1: Definition sketch of the problem.

Our basic equations with  $\lambda$  as the thermal volume expansion,  $\mathbf{u}$  the seepage velocity,  $\mu$  the dynamic viscosity,  $p$  the pressure,  $K$  the permeability ( $K = k_0 e^{kz}$ ),  $C$  the specific heat, and  $\kappa_m$  the overall thermal conductivity, are

**Equation of state:**

$$\rho = \rho_0(1 - \lambda T) \quad (1)$$

**Darcy's law:**

$$\mathbf{u} = -\frac{K}{\mu}(\Delta p - \rho \mathbf{g}) \quad (2)$$

**Incompressible flow:**

$$\nabla \cdot \mathbf{u} = 0 \quad (3)$$

**Energy equation:**

$$(\rho C)_m \frac{\partial T}{\partial t} + (\rho C)_f \mathbf{u} \cdot \nabla T = \kappa_m \nabla^2 T. \quad (4)$$

The basic steady-state solution of the system (1)–(4) satisfying the boundary conditions  $T = T_0 + \Delta T$  at  $z = 0$  and  $T = T_0$  at  $z = h$  is given by

$$\mathbf{u}_b = 0, \quad \frac{\partial}{\partial t} = 0, \quad (5)$$

$$T_b = T_0 + \Delta T \left(1 - \frac{z}{h}\right), \quad (6)$$

$$p_b = p_0 - \rho_0 g \left[ T_0 z + \frac{\lambda \Delta T}{2} \left( \frac{z^2}{h} - 2z \right) \right]. \quad (7)$$

This solution is the conduction state where all the heat is transferred due to thermal conduction.

**2.1 Linear stability analysis**

Now we examine the stability of this solution with the following small perturbation quantities given by

$$\mathbf{u} = \mathbf{u}_b + \mathbf{u}', \quad T = T_b + T', \quad P = p_b + p'. \quad (8)$$

By substituting (8) into Eqs. (2)–(4) and neglecting second-order small quantities, our linearized perturbed equations in dimensionless form (omitting primes) are

$$\nabla \cdot \mathbf{u} = 0 \quad (9)$$

$$0 = -\nabla p - \frac{\mathbf{u}}{K_p} + \text{Ra} \theta \hat{k} \quad (10)$$

$$\frac{\partial \theta}{\partial t} - w = \nabla^2 \theta \quad (11)$$

where  $K_p = f(z) = e^{kz}$  is the permeability of the porous medium, which defines its ability to transmit a fluid. The dimensionless number

$$\text{Ra} = \frac{\rho_f k_0 g \lambda \Delta T h}{\mu \kappa_m}$$

is the Rayleigh number, which is the ratio of buoyancy forces to diffusive resistance.

The component form of Eq. (10) can be written as

$$\frac{u}{f(z)} = -p_x, \quad (12)$$

$$\frac{w}{f(z)} = -p_z + \text{Ra}\theta. \quad (13)$$

As we are looking for the neutral stable case, (11) takes the form

$$-w = \theta_{xx} + \theta_{zz}. \quad (14)$$

Equations (12) and (13) couple the two unknowns  $\theta$  and  $w$  subject to the boundary conditions (both boundaries are impermeable and are perfect thermal conductors):

$$w = \theta = 0, \quad \text{at } z = 0, 1. \quad (15)$$

Now differentiating (12) by  $z$  and (13) by  $x$ , and equating we get

$$\left(\frac{w}{f}\right)_x = \left(\frac{u}{f}\right)_z + \text{Ra}\theta_x \quad (16)$$

Let  $\psi$  be the stream function such that

$$w = -\psi_x \quad \text{and} \quad u = \psi_z. \quad (17)$$

Then (16) becomes

$$\frac{1}{f}(\psi_{xx} + \psi_{zz}) - \frac{f'}{f^2}\psi_z = -\text{Ra}\theta_x \quad (18)$$

and Eq. (14) becomes

$$-\psi_x = \theta_{xx} + \theta_{zz}. \quad (19)$$

Let

$$(\psi, \theta) = (\hat{\psi}, \hat{\theta})e^{iax} \quad (20)$$

and

$$D = \frac{d}{dz}. \quad (21)$$

Equations (18) and (19) become

$$\frac{1}{f} \left( D^2 \hat{\psi} - \frac{f_z}{f} D \hat{\psi} - a^2 \hat{\psi} \right) = -\text{Ra} \hat{\theta}_x \quad (22)$$

and

$$ia \hat{\psi} = (D^2 - a^2) \hat{\theta}. \quad (23)$$

Eliminating  $\hat{\theta}$  from Eqs. (22) and (23),

$$D^4\hat{\psi} - 3kD^3\hat{\psi} + (3k^2 - 2a^2)D^2\hat{\psi} + (3ka^2 - k^3)D\hat{\psi} + (a^4 - a^2k^2 - a^2Ra e^{kz})\hat{\psi} = 0 \tag{24}$$

where we considered permeability of the form  $f(z) = e^{kz}$ . The associated boundary conditions are

$$\begin{aligned} \hat{\psi} &= 0 & \text{at } z &= 0, 1 \\ \hat{\psi}_{zz} - k\hat{\psi}_z &= 0 & \text{at } z &= 0, 1. \end{aligned} \tag{25}$$

### 2.2 Numerical Solution and Graphical Results

We solved fourth-order linear differential equation in  $\hat{\psi}$  (24) subject to the boundary conditions in (25) in Matlab. We used `bvp4c` [2] to solve the boundary value problem. We computed the critical Rayleigh numbers  $Ra_c$  against  $k = -3, -2, -1, 0, 1, 2, 3$ , where  $k = 0$  corresponds to the standard case. The variation of Rayleigh number  $Ra$  against wavenumber  $a$  is shown in Fig. 2 where  $Ra$  is calculated on a logarithmic scale. The variation of critical Rayleigh number  $Ra_c$  for various values of permeability  $k$  is plotted in Fig. 3. As permeability increases, the critical Rayleigh number starts decreasing.

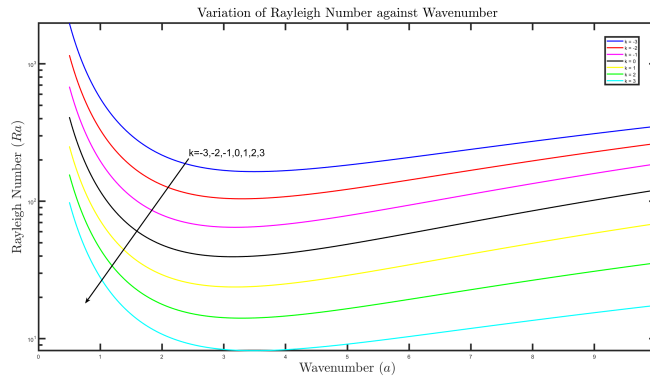


Fig. 2: Variation of Rayleigh numbers against wavenumber.

Table 1: Critical Rayleigh numbers

$k$	Critical Rayleigh number ( $Ra_c$ )	Wave Number ( $a$ )
-3	164.3881	3.4900
-2	104.2661	3.2925
-1	64.6633	3.1790
0	39.4784	$\pi$
1	23.7882	3.1788
2	14.1107	3.2920
3	8.1838	3.4891

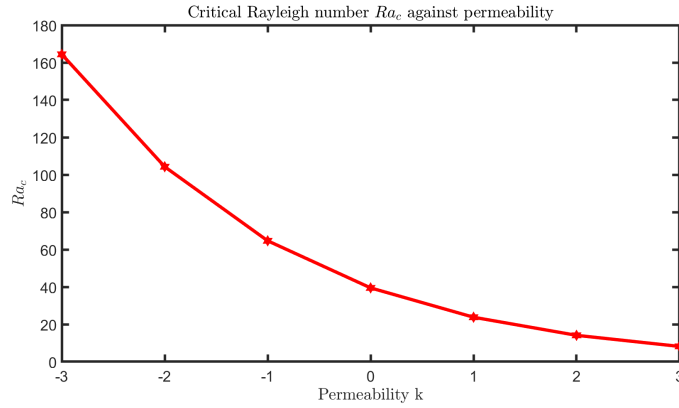


Fig. 3: Variation of permeability against critical Rayleigh number.

If we scale the Rayleigh number based on average permeability, then:

$$Ra_{av} = \frac{\rho_f g \lambda \Delta T h \int_0^1 (k_0 e^{kz}) dz}{\mu \kappa_m} = \frac{\rho_f k_0 g \lambda \Delta T h}{\mu \kappa_m} \left( \frac{e^k - 1}{k} \right) = Ra \left( \frac{e^k - 1}{k} \right), \quad (26)$$

and the critical Rayleigh number  $Ra_{av,c}$  is expressed as:

$$Ra_{av,c} = Ra_c \left( \frac{e^k - 1}{k} \right), \quad (27)$$

where  $Ra_c$  is the critical Rayleigh number given in Table 1.

The critical Rayleigh number  $Ra_{HM,c}$  calculated on the basis of harmonic permeability is expressed as:

$$Ra_{HM,c} = Ra_c \frac{k}{1 - e^{-k}}. \quad (28)$$

We re-scaled the Rayleigh number based on average permeability and harmonic permeability in Eqs. (27) and (28), respectively, to get a fair analysis. Figures 4

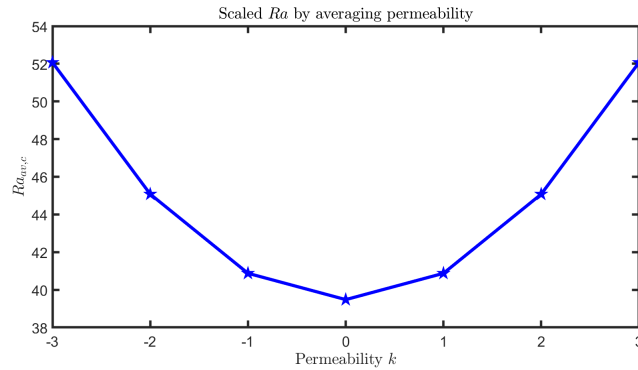


Fig. 4: Variation of  $Ra_{av,c}$  against permeability  $k$ .

and 5 show the variation of the critical Rayleigh number calculated on the basis of average permeability and harmonic permeability respectively. It is interesting to see that the variation of the critical Rayleigh number  $Ra_{av,c}$  and  $Ra_{HM,c}$  is symmetric in each case. Thus for  $Ra < Ra_c$  the conduction state remains stable, and as  $Ra$  is increased above  $Ra_c$ , instabilities cause convection in the form of cellular motion with horizontal wave number  $a$ .

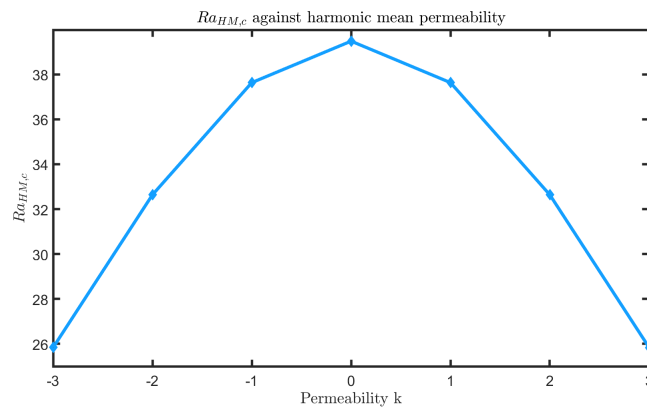


Fig. 5: Variation of  $Ra_{HM,c}$  against permeability  $k$ .

In Fig. 6, we compared flow speed and permeability as a function of height ( $z$ ) along the centre of the convection cell. From Fig. 6(a,c), we conclude the asymmetric trend of the flow and permeability. In Fig. 7, we compared temperature ( $\theta$ ) and permeability as a function of height ( $z$ ) along the centre of the convection cell. Figure 7(a,c), also shows the asymmetric trend of the temperature and permeability.

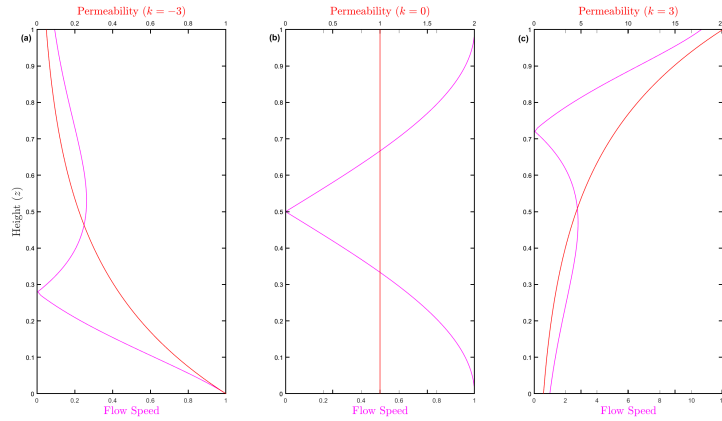


Fig. 6: Comparison of flow speed and permeability as a function of height.

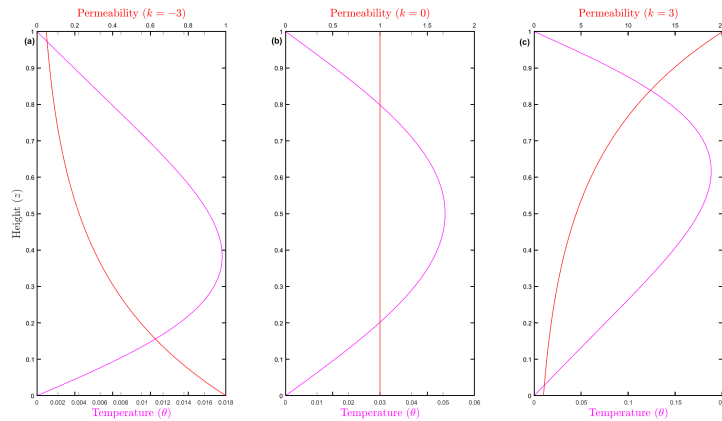


Fig. 7: Comparison of temperature and permeability as a function of height.

The contours for temperature  $\theta(x, z)$  and stream function  $\psi(x, z)$  are plotted in Fig. 8 and Fig. 9, respectively. Here, we considered  $k = -3, 0, 3$  with corresponding critical Rayleigh numbers given in Table 1 to compare our results with the classical case of  $k = 0$ . When  $k = 0$  the rolls for temperature and stream function are perfectly symmetric in Fig. 8(b) and Fig. 9(b) whereas for  $k \neq 0$  in Fig. 8(a,c) and Fig. 9(a,c), the rolls are not symmetric and are focused on either  $z = 0$  for  $k = -3$  or  $z = 1$  for  $k = 3$ . This is because of the change in critical Rayleigh number  $Ra_c$ . Now rocks with high permeability have strong convection and higher velocity of fluid within the porous layer, increasing the dissolution of sediments whereas for less permeable rocks we observe the negative feedback.

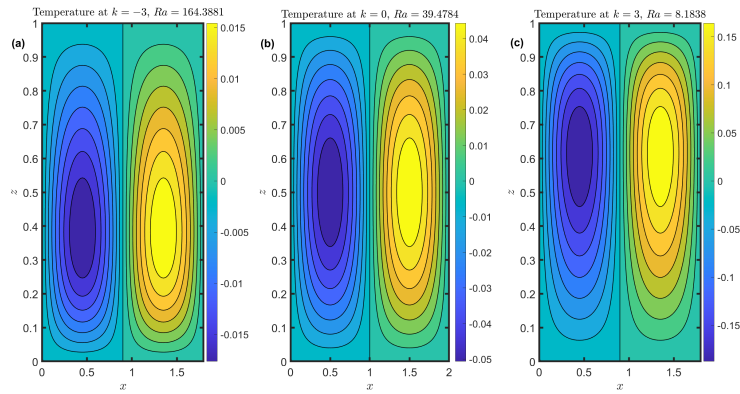


Fig. 8: Variation of temperature against critical Rayleigh number  $Ra_c$  by taking  $k = -3, 0, 3$ .

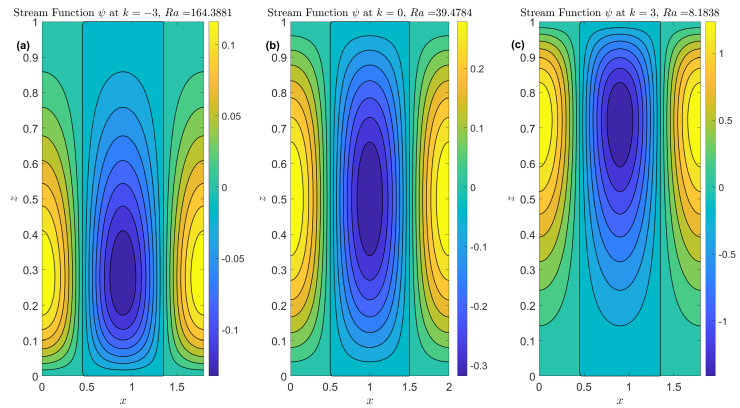


Fig. 9: Variation of stream function  $\psi$  against critical Rayleigh number  $Ra_c$  by taking  $k = -3, 0, 3$ .

### 3 Conclusion

In this study, we analysed the effect of permeability on convection pattern. In pure convection ( $k = 0$ ), conduction is stable for  $Ra < 4\pi^2$  and we have instability in the form of convection rolls as we reach critical Rayleigh number  $Ra_c$ . Permeability has a significant impact on the stability of the conduction state. By examining the depth-averaged permeability, the system exhibits symmetric behaviour for positive and negative values of permeability. The asymmetric behaviour of the convection is evident from flow speed and temperature profiles for  $k > 0$  and  $k < 0$  along the

centre of the convection cell. Thus asymmetric permeability results in asymmetric convection pattern.

## References

1. Ratouis, Thomas MP, and Sadiq J. Zarrouk. Factors controlling large-scale hydrodynamic convection in the Taupo Volcanic Zone (TVZ), New Zealand. *Geothermics* **59**, 236-251 (2016).
2. Jacek Kierzenka (2024). Tutorial on solving BVPs with BVP4C (<https://www.mathworks.com/matlabcentral/fileexchange/3819-tutorial-on-solving-bvps-with-bvp4c>), MATLAB Central File Exchange. Retrieved May 14, 2024.
3. Horton CW, Rogers Jr FT. Convection currents in a porous medium. *Journal of Applied Physics* **16**, 367-70 (1945).
4. Lapwood ER. Convection of a fluid in a porous medium. *Mathematical Proceedings of the Cambridge Philosophical Society* **44**, 508-521 (1948).
5. Nield DA, Bejan A. *Convection in porous media*. New York: Springer (2006).
6. Hewitt DR. Evolution of convection in a layered porous medium. *Journal of Fluid Mechanics* **941**, A56 (2022).
7. Bejan A, Khair KR. Heat and mass transfer by natural convection in a porous medium. *International Journal of Heat and Mass Transfer* **28**, 909-918 (1985).
8. Hewitt DR. Vigorous convection in porous media. *Proceedings of the Royal Society A* **476**, 20200111 (2020).
9. Prasad VF, Kulacki FA, Keyhani M. Natural convection in porous media. *Journal of Fluid Mechanics* **150**, 89-119 (1985).
10. Hardee HC, Nilson RH. Natural convection in porous media with heat generation. *Nuclear Science and Engineering* **63**, 119-132 (1977).